The Transient Impulse Response Modeling Method for Non-parametric System Identification

Per Hägg [a], Johan Schoukens [b], Michel Gevers [c], Håkan Hjalmarsson [a],

[a] *Automatic Control Lab and ACCESS, School of Electrical Engineering, KTH, 100 44 Stockholm, Sweden.*

[b] *Vrije Universiteit Brussel, ELEC Department, Pleinlaan 2, 1050 Brussels, Belgium*

[c] *ICTEAM, Université Catholique de Louvain, B1348 Louvain la Neuve, Belgium*

Abstract

A method for the nonparametric estimation of the Frequency Response Function (FRF) was introduced in [4] and later called Transient Impulse Response Modeling Method (TRIMM). We present here a slightly improved version of the original method and, more importantly, we thoroughly analyze the method in terms of bias and variance errors. This analysis leads to guidelines for the choice of the design parameters in TRIMM. Our theoretical expressions for the bias and variance errors are validated by simulations which, at the same time, highlight the effect of the design parameters on the performance of the method.

Key words: Non-parametric identification. Frequency domain. Identification algorithms.

1 Introduction

Frequency Response Function (FRF) estimation is a classical problem in system identification. The identification method may be either parametric, where the model of the system is parameterized with a finite number of parameters, often considerably less than the number of data points, or non-parametric where the number of parameters are as many as the number of data points. In this paper we will focus on the latter. The non-parametric estimates are often used in the initial stage of the identification process to get insight into various system properties, such as system order and noise characteristics, and can guide the user in the model selection in order to proceed with a more accurate parametric estimate. Non-parametric frequency response functions are also useful in their own right and are used intensively in many engineering fields, for example in audio applications, power systems and vibration analysis.

The classical approach is to use spectral analysis, see, e.g., textbooks like [1], [17], [7], [13]. The idea is to smooth the raw Discrete Fourier transform (DFT) estimate using information from adjacent frequencies, or, equivalently, to use weighting of the correlation estimates of different time-lags.

All nonparametric methods suffer from transient (or leakage) errors and noise errors. Transient errors occur when using a finite number of data and a non-periodic input signal. This has for a long time been a major deterrent against the use of nonparametric estimates of the FRF in the presence of non-periodic input signals.

However, by assuming the system to be finite dimensional the leakage error can be analyzed in detail, see [10], [8]. This analysis indicates that this error is highly structured with a smooth frequency characteristic. In [16] this property is explored to develop what is known as the Local Polynomial Method (LPM), an alternative to the classical frequency smoothing. The idea is to approximate the smooth leakage term by a Taylor series expansion and to simultaneously estimate the coefficients of this expansion together with the frequency response at one frequency at a time. The method has been demonstrated to provide superior accuracy, as compared to traditional smoothing algorithms, on a number of problems, see for example [11,12]. The method has been further developed in [2,9].

Inspired by the LPM method, the Transient and Impulse Response Modeling Method (TRIMM) was introduced in [4]. The leakage error, or transient, is modelled with a

Email addresses: per.hagg@ee.kth.se (Per Hägg), johan.schoukens@vub.ac.be (Johan Schoukens), michel.gevers@uclouvain.be (Michel Gevers), hakan.hjalmarsson@ee.kth.se (Håkan Hjalmarsson).

finite impulse response model. To be able to simultaneously estimate both the FIR parameters and the system frequency response over the grid of DFT frequencies, the DFT of the output measurements have to be recycled and used several times. The main difference compared to LPM is that the transient is globally parameterized as opposed to locally in LPM. The global parameters are then estimated using the whole data record. In LPM only the data points in a local window around each frequency are used to estimate the transient.

Some first attempts to analyze the TRIMM method are given in [3,5]. The objective of this paper is to give a more detailed variance and bias analysis of the method to be able to guide the user in the choice of design parameters and experimental settings. As the general problem, with arbitrary system, input and noise sources is hard to analyze, we will in this paper consider a few special cases. Although the analysis is restricted, this gives some insight into the inner workings of the method and we will discuss the expected implications from this analysis to more general cases. For the bias we will mainly study the errors for second order systems with low damping. The motivation for this choice is that most systems can be written as sums of first and second order systems and that the part with lowest damping introduces the largest bias error [15]. We will also give some results for the case when the system is highly damped.

The main contribution of this paper is first to present the idea behind, and to summarize the previous work related to the TRIMM method. The second contribution is to analyze the bias and variance errors of the estimated frequency response function with TRIMM. This will allow us, in future work, to compare different estimation methods and to give some user guidance on when and how the different methods should be used.

The outline of the rest of the paper is as follows. In Section 2 the frequency domain input-output relation is shown that is then used in Section 3 to derive the TRIMM method. In Section 4, bias and variance expressions for TRIMM are derived. The results and their implications in terms of the design choices of the TRIMM method are discussed in Section 5. The bias and variance expressions are then verified in Monte-Carlo simulations in Section 6 and applied to a vibrating steel beam experimental system in Section 7. Finally, Section 8 concludes the paper.

2 The Input-Output Relation

Consider a linear discrete-time single-input single-output (SISO) system, $G(q)$. The system is excited by an input signal $u(t)$ and the output $y(t)$ is assumed to be disturbed by additive measurement noise $v(t)$. The input-output relation can then be written as

$$y(t) = G(q)u(t) + v(t) \tag{1}$$

where q is the forward shift operator and $G(q)$ is a causal rational function of q.

Equivalently, it can also be represented in state-space form as

$$\begin{aligned} x(t+1) &= Ax(t) + Bu(t), \\ y(t) &= Cx(t) + v(t). \end{aligned} \tag{2}$$

where $x(t)$ is the state vector and $x(0) = x_0$.

Taking the N-point DFT

$$Z(k) = \frac{1}{\sqrt{N}} \sum_{t=0}^{N-1} z(t) e^{-j\omega_k t} \tag{3}$$

of the finite record of measured input and output data $\{u(t)\}$ and $\{y(t)\}$, $t = 0, \ldots, N-1$ gives the following input-output DFT relation [8] for $k = 0, \ldots N-1$

$$Y(k) = G(e^{j\omega_k})U(k) + T(e^{j\omega_k}) + V(k), \tag{4}$$

where $\omega_k \triangleq \frac{2\pi k}{N}$ are the DFT frequencies. The leakage term T is due to the non-zero initial condition and the finite data record length. It is important to understand that (4) is an exact relation between the finite input and output data records [10,8].

To simplify the notation we write the frequency domain expression (4) as

$$Y_k = G_k U_k + T_k + V_k, \quad k = 0, \ldots, N-1$$

where $X_k = X(e^{j\omega_k})$.

It has been shown that the transient term, evaluated at $e^{j\omega_k}$ can be expressed as [8]:

$$\begin{aligned} T_k &= \frac{1}{\sqrt{N}} C(I - e^{-j\omega_k} A)^{-1}(x_0 - x_N) \\ &= \frac{1}{\sqrt{N}} \sum_{t=0}^{N-1} CA^t (I - A^N)^{-1}(x_0 - x_N) e^{-j\omega_k t} \end{aligned} \tag{5}$$

where x_N is the state at time $t = N$ of the state space realization (2). This special structure of the transient is utilized in TRIMM.

Although the method presented in this paper can be applied to both random and deterministic input signals, we will assume that both the input, $u(t)$, and the disturbing noise, $v(t)$, can be described as filtered zero mean noise with existing moments of any order. The DFT of the input and the noise are then asymptotically ($N \to \infty$) independent over the frequencies, circular complex normally distributed [13]. Furthermore we assume that the system operates in open loop and thus $u(t)$ is independent of $v(t)$.

3 The TRIMM Method

The objective is to estimate the Frequency Response Function $G(e^{j\omega_k})$ for the whole frequency grid, $k = 0, \ldots, N-1$. To perform this estimation we utilize the exact relations (4) and also identify the transient term, T. However, since there are only $N/2$ complex equations, it is impossible to directly estimate the N complex unknown parameters $\{G_k, T_k, k = 0, \ldots, N-1\}$. To generate more equations we approximate G_k and T_k in a local window of size $2L+1$ around each frequency ω_k.

To relate the frequency response at frequency ω_k with the frequency response at the neighbouring frequencies $\omega_{k+r}, r = -L, \ldots, L$ we write

$$\begin{aligned} Y_{k+r} &= G_{k+r}U_{k+r} + T_{k+r} + V_{k+r} \\ &= G_kU_{k+r} + [G_{k+r} - G_k]\,U_{k+r} + T_{k+r} + V_{k+r}. \end{aligned} \tag{6}$$

Using the definition of G_k we can now express the difference $G_{k+r} - G_k$ in (6) as

$$\begin{aligned} G_{k+r} - G_k &= \sum_{t=1}^{\infty} g(t)\left(e^{-j\omega_{k+r}t} - e^{-j\omega_k t}\right) \\ &= \sum_{t=1}^{N-1}\sum_{p=0}^{\infty} g(t+pN)\left(e^{-j\omega_{k+r}t} - e^{-j\omega_k t}\right) \\ &\triangleq \sum_{t=1}^{N-1} \tilde{g}(t)\left(e^{-j\omega_{k+r}t} - e^{-j\omega_k t}\right) \end{aligned} \tag{7}$$

where $g(t) \triangleq CA^{t-1}B$ is the impulse response of the system (2) and $\tilde{g}(t) = \sum_{p=0}^{\infty} g(t+pN)$.

The transient term T_{k+r} from (5) can be written as

$$T_{k+r} = \frac{1}{\sqrt{N}} \sum_{t=0}^{N-1} \tau(t) e^{-j\omega_{k+r}t}. \tag{8}$$

where $\tau(t) = CA^t(I - A^N)^{-1}(x_0 - x_N)$.

Approximating (7) and (8) by truncated lower order sums with n_1 and n_2 terms, respectively, and substituting these into (6) we get

$$\begin{aligned} Y_{k+r} \approx\; & G_kU_{k+r} + \frac{1}{\sqrt{N}} \sum_{t=0}^{n_1-1} \tau(t) e^{-j\omega_{k+r}t} \\ & + \left[\sum_{t=1}^{n_2} \tilde{g}(t)\left(e^{-j\omega_{k+r}t} - e^{-j\omega_k t}\right)\right] U_{k+r} + V_{k+r}, \end{aligned} \tag{9}$$

see [5] for details. In each frequency window, $r = -L, \ldots, L$, around the center frequency ω_k the equations in (9) constitute a set of $2(2L+1)$ real equations for the $2 + n_1 + n_2$ real unknown variables G_k, $\{\tau(t), t = 0, \ldots, n_1 - 1\}$ and $\{\tilde{g}(t), t = 1, \ldots, n_2\}$. Note that each complex relation (9) counts for two real equations; note also that G_k is complex and thus counts for 2 unknowns, while the $\tau(t)$ and $\tilde{g}(t)$ are real.

The variables $\tilde{g}(t)$ and $\tau(t)$ are independent of the frequency ω_k and are hence global parameters. The main idea of TRIMM is to setup a global Least Squares problem by assembling the $2N(2L+1)$ real equations (9) for the N DFT frequencies $\omega_0, \ldots, \omega_{N-1}$ in the $2N + n_1 + n_2$ real unknown parameters

$$\begin{aligned} G &\triangleq [G_0, \ldots, G_{N-1}]^T \\ \theta_2 &\triangleq [\tau(0), \ldots, \tau(n_1); \tilde{g}(1), \ldots, \tilde{g}(n_2)]^T. \end{aligned} \tag{10}$$

Stacking the extended input-output relations (9) into vectors gives

$$Y = \Phi_1 G + \Phi_2 \theta_2 + E + V, \tag{11}$$

where the vector E with elements

$$\begin{aligned} E_{k+r} = & \frac{1}{\sqrt{N}} \sum_{t=n_1}^{N-1} CA^t(I - A^N)^{-1}(x_0 - x_N) e^{-j\omega_{k+r}t} \\ & + \sum_{t=n_2+1}^{N-1} \tilde{g}(t)\left(e^{-j\omega_{k+r}t} - e^{-j\omega_k t}\right) U_{k+r} \end{aligned} \tag{12}$$

accounts for the approximation errors due to the truncated sums in (9) and Φ_1 and Φ_2 are appropriate regressor matrices defined in Appendix A.

A least squares estimate of the transfer function G and the surplus variables θ_2 is then

$$\{\hat{G}, \hat{\theta}_2\} = \arg\min_{G,\theta_2} \|Y - \Phi_1 G - \Phi_2 \theta_2\|_2^2. \tag{13}$$

This gives the following estimates

$$\begin{bmatrix} \hat{G} \\ \hat{\theta}_2 \end{bmatrix} = \begin{bmatrix} G^{(0)} \\ \theta_2^{(0)} \end{bmatrix} + \begin{bmatrix} \Phi_1^*\Phi_1 & \Phi_1^*\Phi_2 \\ \Phi_2^*\Phi_1 & \Phi_2^*\Phi_2 \end{bmatrix}^{-1} \begin{bmatrix} \Phi_1^* \\ \Phi_2^* \end{bmatrix} (E + V) \tag{14}$$

where $G^{(0)}, \theta_2^{(0)}$ are the parameters of the true system.

Remark 1 *The least squares problem (13) consists of $2N(2L+1)$ equations in the $2N + n_1 + n_2$ real unknowns, where each G_k counts for 2 real unknowns. Even for modest N and L the direct solution becomes computational prohibitive. However, the problem has a certain structure that can be exploited. In [4] and [5] it is shown how the problem can be solved by solving a series of smaller least squares problem.*

4 Error Analysis

In this section we will study the bias errors due to undermodeling, and the variance errors due to noisy measurements, of the TRIMM method. In both cases, we will go beyond the general formulas by considering special cases for which much more insight can be gained.

4.1 Bias of the frequency response function estimate

Since $E\{V\} = 0$ by assumption, and since Φ_1 and Φ_2 are independent of V, the bias of the estimates (14) can be written as

$$E\left\{\begin{bmatrix}\hat{G}-G^{(0)}\\ \hat{\theta}_2-\theta_2^{(0)}\end{bmatrix}\right\} = \begin{bmatrix}\Phi_1^*\Phi_1 & \Phi_1^*\Phi_2\\ \Phi_2^*\Phi_1 & \Phi_2^*\Phi_2\end{bmatrix}^{-1}\begin{bmatrix}\Phi_1^*\\ \Phi_2^*\end{bmatrix}E$$

where the expected value is taken over the noise realization. We see that the bias is proportional to the approximation error E.

Since θ_2 is a global parameter vector that depends on the complete data record, the calculations become quite involved. To simplify the calculations, we shall analyze only the bias of FRF, $\hat{G}$, and we shall assume in the analysis of the bias that the true values of the surplus parameter vector, $\theta_2^{(0)}$, are known. By using this assumption, the bias can be studied individually in the different frequency windows. Although this assumption seems restrictive, it gives us a good approximation of the order of magnitude of the bias error. Furthermore, simulations will show that the expressions we derive using this assumption approximate the true bias very well. Under this assumption, the bias in the FRF estimate can be written as

$$E\left\{\hat{G}-G^{(0)}\right\} \approx (\Phi_1^*\Phi_1)^{-1}\Phi_1^*E. \tag{15}$$

To obtain more intuition about the bias error, we shall consider separately the case where the dominating dynamics has low damping (poles close to the unit circle), and the case of a highly damped system.

4.1.1 Bias for lightly damped systems

Any linear transfer function can be written as a sum of first-order systems with complex or real poles. If the poles are complex conjugate, their contribution can be written as a second-order transfer function. The total estimation error will be a sum of the error contributions from the different first order systems in the sum. However the general case is hard to analyze and we will instead look at the dominating term of the transfer function in the analysis of the bias *i.e.,* the part of the system containing the pole closest to the unit circle as this will dominate the errors. We will hence assume, without great loss of generality, that the system can be approximated by a second order system with two complex conjugate poles similarly to what was done in [15] where the bias error was analyzed for the Local Polynomial Method.

Thus, consider the discrete time second-order system

$$G(z) = \frac{z}{z^2 - 2\lambda\cos(\omega_n)z + \lambda^2} = \frac{bp}{z-p} + \frac{\bar{b}\bar{p}}{z-\bar{p}} \tag{16}$$

where

$$b = \frac{1}{2j\lambda\sin(\omega_n)},\ p \ = \lambda e^{j\omega_n}.$$

Here $\lambda = 1-\epsilon$ is the magnitude of the complex conjugate poles of the systems and hence ϵ can be seen as the damping of the system or the distance of the poles to the unit circle. The lower the value of ϵ, the more lightly damped the system will be and the higher the resonance peak will be in the resonance frequency ω_n. Here we will study lightly damped systems, *i.e.,* we consider systems with ϵ close to zero. The maximum of the transfer function amplitude is then obtained at the frequencies $\omega = \pm\arccos(\frac{\lambda^2+1}{2}\cos(\omega_n)) \approx \pm\omega_n$. Close to the resonance frequency, ω_n, the first term of (16) dominates and we approximate the system by

$$G(z) \approx \frac{bp}{z-p}, \text{ for } z \approx e^{j\omega_n}. \tag{17}$$

In Figure 1 the amplitude plot of the system (17) is shown. We will see in the following that the $3\,dB$ bandwidth of the resonance peak will play a vital role in the analysis. The definition of the $3\,dB$ bandwidth, $B_{3\text{dB}}$, is the frequency band for which $|G(\omega)| > G_{max} - 3\,dB$, see Figure 1. One can show that for low damping the bandwidth is $B_{3\text{dB}} = 2\epsilon$.

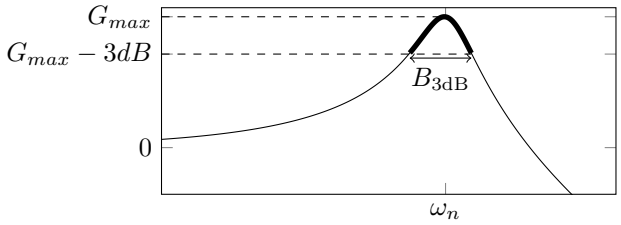

Fig. 1. The definition of the $3\,dB$ bandwidth (in bold) of a normalized second order lightly damped system around the resonance peak at frequency ω_n.

One possible state-space realization of the system (17) around the resonance frequency is $[A, B, C, D] = [p, 1, pb, 0]$. The (complex) impulse response of (17) can be written as

$$g(t) = bp^t = b\lambda^t e^{j\omega_n t} \quad \text{for} \quad t \geq 1.$$

The maximum of the approximation error (12) is obtained at the resonance frequency, *i.e.,* at the frequency $\omega_k = \omega_n$. At this frequency the approximation error is

$$E_{n+r} = \frac{bp}{\sqrt{N}} \frac{1}{1-\lambda^N} \frac{\lambda^{n_1} e^{-j\omega_r n_1} - \lambda^N}{1-\lambda e^{-j\omega_r}} (x_0 - x_N) + \frac{bU_{n+r}}{1-\lambda^N} \left(\frac{\lambda^N - \lambda^{n_2+1}}{1-\lambda} - \frac{\lambda^N - \lambda^{n_2+1} e^{-j\omega_r(n_2+1)}}{1-\lambda e^{-j\omega_r}} \right), \tag{18}$$

see Appendix B for a complete derivation. The first term in (18) stems from the unmodeled dynamics of the transient term while the second term is from the omitted impulse response coefficients. Since the maximum element of E is given in (18) we can already get some insight regarding the bias. For example, if $n_1 = N$ and $n_2+1 = N$, the approximation error will be zero and consequently the bias will be zero.

Inserting the approximation error (18) in (15) and using the structure of Φ_1, the bias at frequency ω_n, $E\left\{\hat{G}_n - G_n^{(0)}\right\}$, can be written as

$$\frac{bp}{\sqrt{N}} \frac{1}{1-\lambda^N} \sum_{r=-L}^{L} \frac{\lambda^{n_1} e^{-j\omega_r n_1} - \lambda^N}{1-\lambda e^{-j\omega_r}} \frac{U_{n+r}^*(x_0 - x_N)}{\sum_{q=-L}^{L} |U_{n+q}|^2} + \sum_{r=-L}^{L} \frac{b}{1-\lambda^N} \left(\frac{\lambda^N - \lambda^{n_2+1}}{1-\lambda} - \frac{\lambda^N - \lambda^{n_2+1} e^{-j\omega_r(n_2+1)}}{1-\lambda e^{-j\omega_r}} \right) \cdot \frac{|U_{n+r}|^2}{\sum_{q=-L}^{L} |U_{n+q}|^2}, \tag{19}$$

where the terms corresponds to the unmodeled transient elements and the unmodeled impulse response elements, respectively. See Appendix D for details.

To further simplify the calculations of the bias we will make two assumptions.

Assumption 2 *The local frequency window width L in (9) is small compared to the number of samples, N.*

This assumption is not really restrictive since this is a common choice of the design parameters in practice.

The bias (19) depends on the input signal $u(t)$ (through U_{n+r} and x_N) used during the experiment. It is hard to say more about the bias for a general input signal and we will therefore only look at the case when the input is a stationary stochastic process. This is still a fairly large class of signals and is common in practice. Thus we make the following assumption about the input signal.

Assumption 3 *The input signal spectrum, U_k, is independent over the frequencies, circular complex normally distributed with variance $E\{|U_k|^2\} = \sigma_u^2(k)$. Furthermore, the spectrum is sufficiently smooth so that $\sigma_u^2(n) \approx \sigma_u^2(n+r)$ for $r = -L, \ldots, L$ for L not too large.*

This assumption is fulfilled if the input $u(t)$ is white Gaussian noise, or asymptotically fulfilled (for $N \to \infty$) if the input is filtered white noise [13]. Under Assumptions 2 and 3 and taking the expected value over the input realizations, the bias (19) can be simplified. The results are summarized in Theorem 4. The notation $O(x)$ should be interpreted as a function that tends to zero at least as fast as x.

Theorem 4 (Bias for lightly damped systems) *Under Assumptions 2 and 3, the maximum bias (19) introduced by the approximation error is of the order*

- *If $B_{3dB} < \frac{2\pi}{N}$*

$$E\{\hat{G}_n - G_n^{(0)}\} \approx O\left(\frac{N-n_1}{NB_{3dB}}\right) + O\left(\frac{N-(n_2+1)}{NB_{3dB}}\right)$$

- *If $B_{3dB} > B_{TRIMM}$.*

$$E\{\hat{G}_n - G_n^{(0)}\} \approx \lambda^{n_1} O\left(\frac{1}{NB_{3dB}^2}\right) + \frac{\lambda^N - \lambda^{n_2+1}}{1-\lambda^N} O\left(\left(\frac{B_{TRIMM}}{B_{3dB}}\right)^2\right)$$

Here $B_{TRIMM} \triangleq 2L\frac{2\pi}{N}$ is the frequency width of the local window used in TRIMM *and $B_{3dB} \triangleq 2\epsilon$ is the $3\,dB$ bandwidth of the system with resonance frequency ω_n, see Figure 1. The expectation is taken over both the noise and the input realizations. In both cases, the leftmost terms stem from the undermodelling of the transient while the right terms are due to the undermodeling of the impulse response.*

PROOF. *See Appendix D.*

The first case when $B_{3\text{dB}} < 2\pi/N$ corresponds to the situation where only one frequency point of the local window used in TRIMM is within the $3\,dB$ bandwidth of the resonance peak. The intuition behind the results in this case is as follows.

Assume for simplicity that $|U_k|^2 = 1$ for all k. The bias of the estimate of the frequency response $\hat{G}_n$ due to the truncation of the impulse response can then be written as

$$E\left\{\hat{G}_n - G_n^{(0)}\right\} = \sum_{r=-L}^{L} E_{n+r} \frac{|U_{n+r}|^2}{\sum_{q=-L}^{L} |U_{n+q}|^2} = \frac{1}{2L+1} \sum_{r=-L}^{L} \left(\tilde{G}_{n+r} - \tilde{G}_n\right)$$

where $\tilde{G}_k = \sum_{t=n_2+1}^{N-1} \tilde{g}(t)e^{-j\omega_k}$ is the truncated frequency response. Note that the principal shape of the true system $G^{(0)}$ and the truncated system $\tilde{G}$ are the same, for example they both have their maximum at the same frequency, ω_n. Since we only have one frequency point in the $3\,dB$ bandwidth, we have $\tilde{G}_{n+r} \ll \tilde{G}_n$ for $r \neq 0$ because $\tilde{G}_n$ is at the resonance peak. The bias due to the truncation of the impulse response then becomes

$$\begin{aligned} E\left\{\hat{G}_n - G_n^{(0)}\right\} &= \frac{1}{2L+1}\sum_{r=-L}^{L}\left(\tilde{G}_{n+r} - \tilde{G}_n\right) \\ &\approx \frac{2L}{2L+1}\tilde{G}_n \approx \tilde{G}_n. \end{aligned} \tag{20}$$

The proof of Theorem 4 shows that $\tilde{G}_n \sim O\left(\frac{N-(n_2+1)}{NB_{3\text{dB}}}\right)$ and this gives the resulting bias. The bias is in this case (almost) independent of L and is given by the frequency response of the unmodeled dynamics at the resonance frequency. The intuition is that the extra terms we add by increasing L are much smaller that the point at the resonance frequency. Note that if n_2 is not to large then the bias error is in the same order of magnitude as the resonance peak and we cannot infer anything about the system. Thus, this case should be avoided in practice. The same reasoning holds for the bias due to the truncated transient terms but with the difference that the sum is of the form

$$E\left\{\hat{G}_n - G_n^{(0)}\right\} \approx \frac{1}{2L+1}\sum_{r=-L}^{L}\tilde{T}_{n+r}.$$

where $\tilde{T}_{n+r}$ is the truncated transient term,

$$\tilde{T}_{n+r} = \frac{1}{\sqrt{N}}\sum_{t=n_1}^{N-1}\tau(t)e^{-j\omega_{n+r}t}.$$

Again the transient has a maximum at the resonance frequency ω_n and $T_{n+r} \ll T_n$ for $r \neq 0$. The bias of $\hat{G}_n$ due to the truncation of the transient term can then be written as

$$E\left\{\hat{G}_n - G_n^{(0)}\right\} \approx \frac{1}{(2L+1)}\sum_{r=-L}^{L}\tilde{T}_{n+r} \approx \frac{1}{(2L+1)}\tilde{T}_n.$$

Again, in the proof of Theorem 4 it is shown that $T_n \sim O\left(\frac{N-n_1}{NB_{3\text{dB}}}\right)$. The difference in the results between the bias introduced by the truncation of the impulse response and the transient is due to the different ways they are estimated.

The second case is when $B_{3\text{dB}} > B_{\text{TRIMM}}$, that is, all the $2L+1$ frequency points in the local window of TRIMM are within the $3\,dB$ bandwidth of the resonance peak. Here the bias due to the undermodelling of the transient term depends on $\frac{1}{B_{3\text{dB}}^2}$ and the bias from the impulse response is proportional to $\left(\frac{B_{\text{TRIMM}}}{B_{3\text{dB}}}\right)^2$. The bias is hence decreasing for decreasing local window width L, for increasing number of samples N, and for higher $B_{3\text{dB}}$ bandwidth (lower resonance peak). The proof shows that for $B_{3\text{dB}} > B_{\text{TRIMM}}$, the contribution of the neglected impulse response coefficients to the error $\tilde{G}_{n+r} - \tilde{G}_n$ can be approximated as

$$\tilde{G}_{n+r} - \tilde{G}_n \sim \frac{1}{\varepsilon^2}\sum_{m=1}^{\infty}\frac{\omega_r^m}{m!}$$

The bias error due to the approximation of the impulse response can then be written as

$$\begin{aligned} E\left\{\hat{G}_n - G_n^{(0)}\right\} &= \sum_{r=-L}^{L}\left(\tilde{G}_{n+r} - \tilde{G}_n\right)\frac{|U_{n+r}|^2}{\sum_{q=-L}^{L}|U_{n+q}|^2} \\ &= \frac{1}{2L+1}\sum_{r=-L}^{L}\sum_{m=1}^{\infty}\frac{\omega_r^m}{m!\varepsilon^2} = \frac{1}{(2L+1)}\sum_{r=-L}^{L}\sum_{m=1}^{\infty}\frac{\omega_r^{2m}}{2m!\varepsilon^2} \\ &\approx \frac{1}{(2L+1)\varepsilon^2}\sum_{r=-L}^{L}O\left(\omega_r^2\right) = O\left(\left(\frac{B_{\text{TRIMM}}}{B_{3\text{dB}}}\right)^2\right) \end{aligned} \tag{21}$$

The terms for odd m have disappeared because the sum is symmetric around zero. The proof for the transient error is based on a similar observation.

Note that the result above only holds when $|U_{n+r}|^2$, or $\sigma_u^2(n+r)$, are symmetric around the frequency ω_n. If the input spectrum is not symmetric, the even terms do not disappear and the dominating terms will instead be $O\left(\frac{B_{\text{TRIMM}}}{B_{3\text{dB}}^2}\right)$ for the contribution to the neglected impulse response terms and $O\left(\frac{2L+1}{NB_{3\text{dB}}^2}\right) = O\left(\frac{B_{\text{TRIMM}}}{B_{3\text{dB}}}\right)$ for the transient error. Thus, the bias error due to the neglected impulse response elements is $O(\frac{L}{N})$: the larger the window, the larger the bias error. Similar results for the bias were obtained in [3] for general (higher order) systems.

If the parameters and the system are such that $\frac{2\pi}{N} < B_{3\text{dB}} < B_{\text{TRIMM}}$, then a few but not all points in the local bandwidth of TRIMM is in the $3\,dB$ bandwidth of the system. The bias will then be an interpolation between the results when all points in the local window of TRIMM are within the $3\,dB$ bandwidth and when only one point is within the bandwidth. This can be seen as follows. Introduce the constant $L_{eff} < L$ that represents the number of points within the $3\,dB$ bandwidth. Then the bias from the undermodeling of the impulse

response is proportional to

$$\sum_{r=-L}^{L}\left(\tilde{G}_{n+r}-\tilde{G}_n\right)\approx\sum_{r=-L_{eff}}^{L_{eff}}\left(\tilde{G}_{n+r}-\tilde{G}_n\right)$$

Hence this bias error will mainly be dominated by the points within the $3\,dB$ bandwidth of the system and will be the same as (21), save that L is replaced by L_{eff}. The main result from this section is hence that the number of points used in the local window in TRIMM that are within the $3\,dB$ bandwidth of the system affects the bias to a large extent.

We will discuss the results and consequences in more detail in Section 5.

4.1.2 Bias for highly damped systems

We now study the bias error for the situation where the system is highly damped. Instead of the second order system (16) we now consider a first order discrete time stable system with impulse response $g(t)=\alpha\lambda^t$ where α is a real constant and λ is the real positive pole of the system. Further we consider the highly damped case, *i.e.,* when $\lambda\ll 1$. Much of the analysis can be carried over, save for the difference in damping. Redoing the analysis for this case results in the following theorem.

Theorem 5 (Bias for highly damped systems) *For a system $G(z)$ with impulse response $g(t)=\alpha\lambda^t$, with $0<\lambda\ll 1$ and where α is a constant, the bias introduced by the approximation error (12) is given by*

$$E\{\hat{G}_k-G_k^{(0)}\}\approx\lambda^{n_1}O\left(\frac{1}{N}\right)+\lambda^{n_2+1}O\left(B_{TRIMM}^2\right).$$

PROOF. See Appendix E.

It can be seen that the results for the highly damped case are consistent with the results from the lightly damped case, except that the damping ϵ does not appear in the highly damped case. This is due to the assumption that $\lambda=1-\epsilon\ll 1$.

4.2 Variance of the FRF estimate

In this section we study the variance of the estimates $\hat{G}$ of the frequency response caused by the measurement noise V. To get some insight into the problem and to make it computationally tractable, we look at a few special cases. At the end of this section the implications for the general case will be discussed. In this subsection we will study the how the variance of the frequency response is affected by the choice of the design parameters L, n_1 and n_2 and hence we will no longer assume that the surplus variables θ_2 are known.

First we assume that $v(t)$ is zero mean white noise with variance σ_v^2. Then the covariance matrix of the estimated frequency response and surplus variables (14) around the bias is given by

$$E\left\{\begin{bmatrix}\hat{G}+G^b-G^{(0)}\\ \hat{\theta}_2+\theta_b-\theta_2^{(0)}\end{bmatrix}\begin{bmatrix}\hat{G}+G^b-G^{(0)}\\ \hat{\theta}_2+\theta_b-\theta_2^{(0)}\end{bmatrix}^*\right\}=\begin{bmatrix}\Phi_1^*\Phi_1 & \Phi_1^*\Phi_2\\ \Phi_2^*\Phi_1 & \Phi_2^*\Phi_2\end{bmatrix}^{-1}\sigma_v^2.$$

where G^b and θ_b are the bias in the frequency response function and the surplus variables, respectively. The variance of the FRF estimate can then be written as

$$\begin{aligned}&E\left\{(\hat{G}+G^b-G^{(0)})(\hat{G}+G^b-G^{(0)})^*\right\}\\&=\left(\Phi_1^*\Phi_1-\Phi_1^*\Phi_2\left(\Phi_2^*\Phi_2\right)^{-1}\Phi_2^*\Phi_1\right)^{-1}\sigma_v^2.\end{aligned}\tag{22}$$

We now argue that if the design variables n_1 and n_2 are chosen small then $\Phi_1^*\Phi_1\ \gg\Phi_1^*\Phi_2\left(\Phi_2^*\Phi_2\right)^{-1}\Phi_2^*\Phi_1$ and that, as a result,

$$E\left\{(\hat{G}+G^b-G^{(0)})(\hat{G}+G^b-G^{(0)})^*\right\}\approx\left(\Phi_1^*\Phi_1\right)^{-1}\sigma_v^2.$$

We split the regressor matrix Φ_2, into two parts $\Phi_2=[\Phi_a\,\Phi_b]$ where Φ_a is the part that corresponds to the transient terms, and hence contains no input signals, and where Φ_b is the part related to the impulse response coefficients. We first look at the case when $n_2=0$, *i.e.,* $\Phi_2=\Phi_a$, and we only estimate the transient terms. Then all elements of $\Phi_a\left(\Phi_a^*\Phi_a\right)^{-1}\Phi_a^*$ satisfy

$$\left|\left[\Phi_2\left(\Phi_2^*\Phi_2\right)^{-1}\Phi_2^*\right]_{k,l}\right|\le\frac{n_1}{(2L+1)N}.$$

Due to space limitations, the details are left out but can be found in [6]. Since the rows of Φ_1 only have $(2L+1)$ non-zero elements, *cf.,* (A.1), and these elements are independent of N, we can always choose N large enough so that $\Phi_1^*\Phi_1\ \gg\Phi_1^*\Phi_2\left(\Phi_2^*\Phi_2\right)^{-1}\Phi_2^*\Phi_1$.

We now instead consider the case when $n_1=0$ and only the impulse response coefficients are estimated. We assume that the input, $u(t)$, is white Gaussian noise with variance σ_u^2. In [6] it is shown that the elements of $\Phi_b^*\Phi_b$ are, in this special case, given by

$$[\Phi_b^*\Phi_b]_{m,l}=Nr_u(m-l)\sum_{r=-L}^{L}\left(1-e^{-j\omega_r m}\right)\left(1-e^{j\omega_r l}\right),\tag{23}$$

where $r_u(\tau) = \frac{1}{N}\sum_{t=0}^{N-1} u_t u_{t-\tau}$ is the sample autocorrelation of the input. Since we have assumed that $u(t)$ is white, for large N we have $r_u(m-l) \approx 0$ if $m \neq l$ and $\Phi_b^*\Phi_b$ becomes diagonal. It is then possible to bound the elements of $\Phi_1^*\Phi_2\left(\Phi_2^*\Phi_2\right)^{-1}\Phi_2^*\Phi_1$ as

$$\left|\left[\Phi_1^*\Phi_2\left(\Phi_2^*\Phi_2\right)^{-1}\Phi_2^*\Phi_1\right]_{m,l}\right| \leq$$
$$\left|\frac{3n_2}{N\sigma_u^2(2L+1)}\sum_{r=-L}^{L}|U_{l+r}|^2\right|\sum_{q=-L}^{L}|U_{m+q}|^2 =$$
$$\left|\frac{3n_2}{(2L+1)}\sum_{r=-L}^{L}\frac{|U_{l+r}|^2}{\sum_{k=0}^{N-1}|U_k|^2}\right|\sum_{q=-L}^{L}|U_{m+q}|^2.$$

Again the details are left out but a complete derivation is given in [6]. Since the input $u(t)$ is white and $L \ll N$, the ratio $\frac{|U_{l+r}|^2}{\sum_{k=0}^{N-1}|U_k|^2}$ is small with high probability and goes to zero as N goes to infinity. Furthermore, since $\Phi_1^*\Phi_1$ is diagonal with elements

$$[\Phi_1^*\Phi_1]_{m,m} = \sum_{q=-L}^{L}|U_{m+q}|^2$$

we have, for large enough N, that

$$\Phi_1^*\Phi_1 \gg \Phi_1^*\Phi_2\left(\Phi_2^*\Phi_2\right)^{-1}\Phi_2^*\Phi_1.$$

Hence we have shown in the two cases that, if N is large enough and n_1 and n_2 are small, we can approximate the variance of the frequency response function estimate $\hat{G}$ as

$$E\left\{(\hat{G}+G^b-G^{(0)})(\hat{G}+G^b-G^{(0)})^*\right\} \approx \left(\Phi_1^*\Phi_1\right)^{-1}\sigma_v^2$$
$$= diag\left\{\frac{\sigma_v^2}{\sum_{r=-L}^{L}|U_{0+r}|^2},\ldots,\frac{\sigma_v^2}{\sum_{r=-L}^{L}|U_{N-1+r}|^2}\right\} \quad (24)$$

If the input is smooth over the $2L$ neighbours, expression (24) shows that the variance of the FRF is proportional to $\frac{1}{2L+1}\frac{\sigma_v^2}{\sigma_u^2}$. The variance of $\hat{G}$ is thus proportional to the noise variance and inversely proportional to the input power in the local bandwidth used in TRIMM. A wider bandwidth hence gives lower variance, which is a very intuitive result. Note that the variance of $\hat{G}$ does not decrease with increasing N, since adding more data points also adds more G_k to be estimated.

Now consider the variance of the n_1 and n_2 global parameters $\tau(t)$ and $\tilde{g}(t)$ (defined in (7) and (8)). Unlike the estimate of the frequency response function G_k these parameters are estimated using N data points. As a result their variance can be approximated as [3]

$$E\left\{(\hat{\theta}+\theta_b-\theta_0)(\hat{\theta}+\theta_b-\theta_0)^*\right\} = O\left(\frac{n_1+n_2}{N}\right)\frac{\sigma_u^2}{\sigma_v^2}$$

If n_1 and n_1 are much smaller than the number of samples N the variance of the estimate of the global parameters are small and can be considered known in the estimation of the frequency response. This explains the derived result.

However, the above reasoning only holds if the variance of the surplus variables is small. We see that $\Phi_2^*\Phi_2$ in (23) depends on the correlation properties of the input signal. For example, if the signal is highly correlated, then $\Phi_2^*\Phi_2$ could be close to singular. The inverse will hence be large and the estimate of the frequency response function will be affected, *cf.,* (23). If n_1 and n_2 are of the same order as the number of samples N, the variance of the global parameters will also affect the variance of the FRF estimate.

However, in practice we have observed that these results seem to be good approximations of the variance even for quite small N and for other types of input spectra than considered here.

Finally, if the input is a stochastic process satisfying Assumption 3, then using Lemma 6 in the Appendix shows that the expected variance can be written as

$$E\left\{|\hat{G}_k+G^b-G_k^{(0)}|^2\right\} = \frac{1}{2L}\frac{\sigma_v^2}{\sigma_u^2}, \quad (25)$$

where the expectation is now also taken over the input realization.

5 Discussion

In this section we will summarize and discuss the implications of the main results derived in the previous sections.

- The bias errors for second order systems with low damping and for a first order system with high damping have been calculated in Section 4. The motivation was that many systems can be written as a sum of first and second order contributions by a partial fraction decomposition and that the part with lowest damping dominates the bias error. Of course, if the term with lowest damping has a small amplitude compared to the other terms, this will not dominate the error. Instead the bias should be considered as a function of the frequency where the bias in each frequency is decided by the local dominating system. The derived

results are hence not only valid for the resonance frequency of the system but can be used to gain insight into the bias for the whole frequency response. We also saw that similar results were obtained for the high and low damping case indicating that the results are more general than shown here. The main observation is that the bias is to a large extent decided by the relation between the local bandwidth used in TRIMM and the perceived $3\,dB$ bandwidth in the local frequency window.

- Looking at the approximation error term (12) which represents the unmodeled dynamics, we observe that the choice $n_1 = N$ and $n_2 = N - 1$ gives zero approximation error and consequently an unbiased estimate of the frequency response function. However, this will increase the variance of the estimate considerably.
- Increasing the number of samples N reduces the bias since the local bandwidth used in TRIMM, B_{TRIMM}, is inversely proportional to N. If we are in the situation that $B_{3\text{dB}} < 2\pi/N$, then the bias is not affected much by the number of samples N. However, by increasing N, eventually $B_{3\text{dB}} < 2\pi/N$ will not hold and the bias will decrease as the number of samples is increased. The variance of the FRF estimate is not directly influenced by the number of samples as long as $n_1, n_2 \ll N$. However, by increasing the number of samples we can increase n_1, n_2 making the bias smaller without changing the variance.
- The variance error of $\hat{G}$ is inversely proportional to the local window width L since $2L+1$ data are used in each local window to estimate the frequency response function. Thus, if the noise dominates, one should choose a larger window width.
- The bias expressions derived in Section 4 are based on the assumption that the input spectrum is symmetric around the resonance peak. These results should hold also for non-stochastic input signals as long as they are symmetric around the resonance. For non-symmetric signals the results are no longer valid. The convergence rate will in this case be reduced with one order, for example $O((B_{\text{TRIMM}}/B_{3\text{dB}})^2)$ will now be $O(B_{\text{TRIMM}}/B_{3\text{dB}}^2)$. These results are similar to the bias expressions for more general model structures derived in [3].
- It is seen in Theorem 4 that the bias is lower if L is chosen such that the local bandwidth, $B_{\text{TRIMM}} = 2L\frac{2\pi}{N}$ is within the $3\,dB$ bandwidth of the system. The case when only one point in TRIMM is within the $3\,dB$ bandwidth should be avoided in practice. From equation (20) we have that the bias of the estimate of the frequency response function due to the undermodeling of the impulse response was

$$E\left\{\hat{G}_n - G_n^{(0)}\right\} \approx \tilde{G}_n.$$

Hence, the bias is in the same order as the true system $G^{(0)}$ and there is basically no information about the true system in the estimate. Therefore it is recommended that L should be chosen such that $B_{\text{TRIMM}} < B_{3\text{dB}}$.

Often the exact location of the resonance frequency ω_n of the continuous time system under consideration is a priori unknown. In the bias expressions we have derived we have considered the case when the frequency grid is such that we have one data point exactly at the resonance frequency. If this is not the case, the bias error at the resonance frequency will of course be larger. This further strengthen the recommendation that in practice one should choose the frequency resolution in the experiment such that at least a few frequency points are available in the $3\,dB$ bandwidth of the system in order to have one frequency point sufficiently close to the resonance frequency.

From the above recommendations it is possible to give a lower bound on the required measurement time. If we want $B_{\text{TRIMM}} < B_{3\text{dB}}$ then

$$2L\frac{2\pi}{N} < B_{3\text{dB}} \Leftrightarrow$$
$$N > \frac{4\pi L}{B_{3\text{dB}}} = \frac{2\pi L}{\epsilon} = \frac{2\pi L}{1-\lambda}$$

Since $L \geq 1$ the lower bound is $N \geq \frac{2\pi}{1-\lambda}$.

- Without any windowing there would be fewer equations than unknowns. Assuming that $N > (n_1+n_2)/4$, we observe that choosing $L = 1$ already gives more equations than unknowns. Increasing L above this value decreases the variance as shown in Section 4.2, but it increases the bias as shown in Theorem 4.
- The parameters $\tilde{g}(1), \ldots, \tilde{g}(n_2)$ are only needed to produce approximations of $G_{k+r} - G_k$ in the window around the frequency k. If this window is chosen narrow (*i.e.,* L small) then G_{k+r} is close to G_k and the approximation need not be as precise as when L is large, so that n_2 can also be chosen small.
- From the previous results it is clearly seen that the design parameter L is a trade-off between bias and variance of the estimate of the frequency response. Further insight into the working of the method can be gained by looking at the extreme cases when $L = 0$ and $L = N/2$, *i.e.,* the case when no smoothing is used and the case when all available frequencies are used in every local window, respectively. These two cases were studied in [5].

The results were that TRIMM for the case $L = 0$ boils down to the well known empirical transfer function estimate (ETFE) [7]. If the input is a realization of a stochastic process then the ETFE is an asymptotically unbiased estimate of the transfer function but the variance of the estimate does not decrease as the number of samples N increases [7].

When $L = N/2$ is used the method basically corresponds to estimating a FIR-model for each frequency, see [5] for details. The parameter L can thus not only be seen as a smoothing factor but will also change the method from a fully nonparametric method for $L = 0$

to a parametric FIR-estimation method for $L = N/2$.

6 Simulations

In this section the expressions for the bias and the variance of the TRIMM method will be verified by simulations.

6.1 Bias errors

The first simulations will verify the bias expressions of Theorems 4 and 5. Three different experiments will be carried out where, respectively, the damping ϵ, the ratio $B_{\text{TRIMM}}/B_{\text{3dB}}$ and the user parameters n_1, n_2 are varied. 500 Monte-Carlo simulations are performed for each of the three experiments and the settings used are $N = 1000$ and $\omega_n = 125 \cdot 2\pi/N$.

6.1.1 Varying the damping

First the damping factor, and consequently the $3\,dB$ bandwidth, of the second order system is varied between $10^{-4.5}$ and $10^{-0.5}$. The settings for TRIMM during the experiment are $L = 2$ and $n_1 = n_2 = 20$. Since we know the true underlying system we can separate the bias contribution from the unmodeled dynamics of the transient from the bias contribution from the unmodeled impulse response coefficients in the total bias error. Figure 2a shows the bias contribution from the unmodeled dynamics in the transient from the simulation and the corresponding theoretical values from Theorem 4.Correspondingly, Figure 2b shows the bias contribution from the unmodelled impulse response coefficients. From the figures it is seen that the theoretical decay of the bias error when the damping is increased, closely matches the simulated bias.

6.1.2 Keeping L/B_{3dB} constant

Next the ratio L/ϵ, and consequently $B_{\text{TRIMM}}/B_{\text{3dB}}$, is kept constant. The parameters are selected such that $B_{\text{3dB}} > B_{\text{TRIMM}}$, as this is the interesting case in practice. The local bandwidth L of the TRIMM method is varied between 2 and 20 and the damping is changed as $\epsilon = 10^{-2} \cdot L$. Again we set $n_1 = n_2 = 20$. The simulated bias contributions from the transient and the impulse response are shown in Figure 3 and are again compared to the theoretical values from Theorem 4. As expected from the theory, the contribution from the transient response is relatively unchanged from when only the damping ϵ was varied, *cf.*, Figure 2a as the first term in Theorem 4 is independent of L.

For the bias contribution from the impulse response we expect that when the damping and L are increased the decay should be much smaller since $B_{\text{TRIMM}}/B_{\text{3dB}}$ is constant. The resulting bias is however not expected to

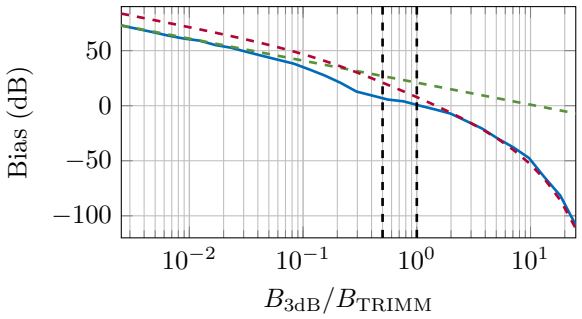

(a) Bias due to undermodeling of transient response.

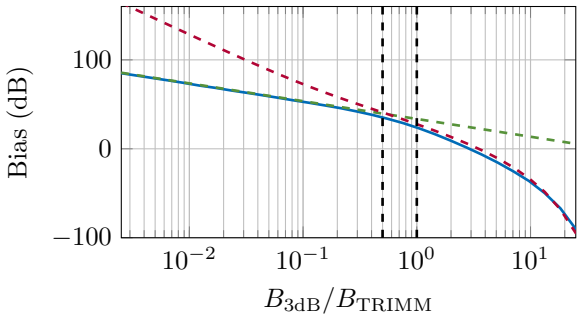

(b) Bias due to undermodeling of impulse response.

Fig. 2. Bias error for second order lightly damped system. Simulated bias error (——) and the theoretical values from Theorem 4 are shown as (- - -) and (- - -). The bounds for which the different terms are valid ($B_{\text{3dB}} < \frac{2\pi}{N}$ and $B_{\text{3dB}} > B_{\text{TRIMM}}$) are shown as (- - -).

be constant since the bias still decays as λ^{n_2+1}, which is a function of the damping ϵ. This is seen in the simulated results in Figure 3.

6.1.3 User design parameters n_1 and n_2

According to Theorem 4, the bias error should decay exponentially as the user design parameters n_1 and n_2 are increased as λ^{n_1+1} and λ^{n_2+1}. To verify this we set $\epsilon = 5 \cdot 10^{-2}$ (such that $B_{\text{TRIMM}} < B_{\text{3dB}}$), $L = 2$ and gradually increase n_1 and n_2 from 5 to 200. The resulting bias errors are shown in Figure 4 together with the theoretical values from Theorem 4. Again, the theoretical and the simulated results are consistent.

6.2 Variance Errors

To verify the variance expression from Section 4.2 the following simple FIR system is studied

$$G(z) = 0.8z^{-1} + 0.6z^{-2} - 0.3z^{-3}.$$

Since we are only interested in the variance error we start by setting $n_1 = n_2 = 3$ in which case we get no bias errors. A zero mean white Gaussian noise input with variance $\sigma_u^2 = 1$ is used as input and $N = 1000$

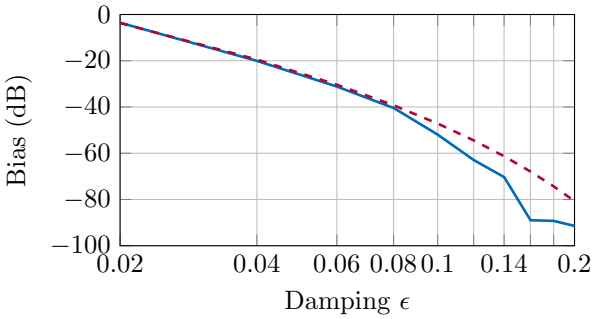

(a) Bias due to undermodeling of transient response.

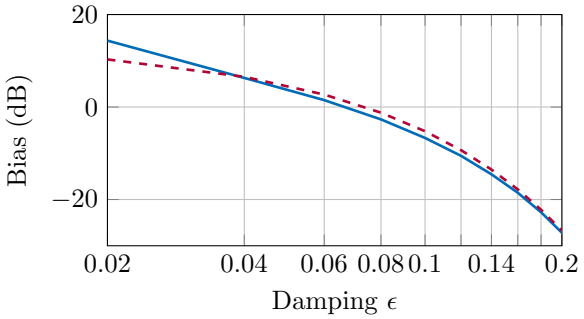

(b) Bias due to undermodeling of impulse response.

Fig. 3. Bias error for second order lightly damped system when $B_{\text{TRIMM}}/B_{3\text{dB}}$ is kept constant. Simulated bias error (——) and the theoretical values from Theorem 4 are shown as (- - -).

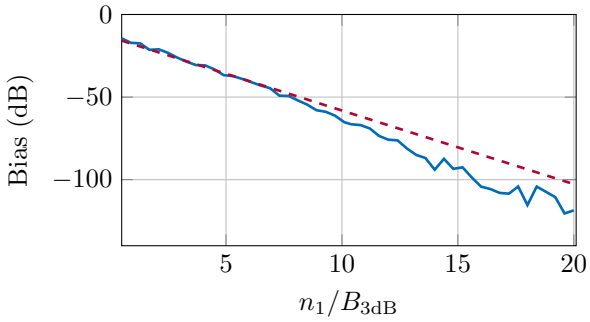

(a) Bias due to undermodeling of transient response.

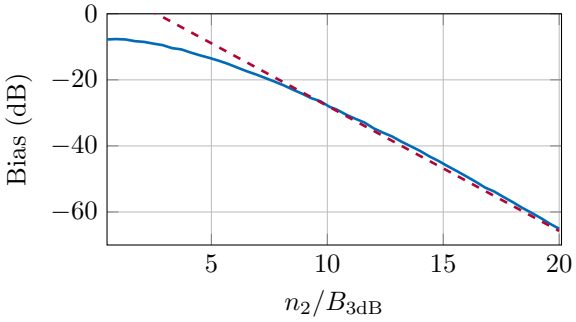

(b) Bias due to undermodeling of impulse response.

Fig. 4. Bias error for second order lightly damped system when the user parameters n_1 and n_2 are increased. Simulated bias error (——) and the theoretical values from Theorem 4 are shown as (- - -).

data points are collected. The output is disturbed with Gaussian white noise with variance $\sigma_v^2 = 0.25$. The local window used by TRIMM, L, is varied as $L = [1, 2, 4, 8, 16]$ and the variance of the estimation error of the FRF is calculated over 500 Monte-Carlo simulations with a new realization of the input and the noise in each iteration. Since $n_1, n_2 \ll N$ we expect that the variance should be

$$E|\hat{G}_k - G_k^{(0)}|^2 \approx \frac{\sigma_v^2}{\sigma_u^2}\frac{1}{2L}. \tag{26}$$

In Figure 5 the simulation results and the theoretical values are shown. We note that the simulated variance error is closely matched by the theory.

In Section 4.2 we concluded that for small n_1 and n_2 the variance of the FRF will be unaffected by n_1 and n_2. Next we look at how large the parameters n_1 and n_2 can be chosen before the variance of the FRF is affected. We use the same settings as before, but now for a fixed $L = 3$. Instead we vary $n_1 = n_2$ from 3 to 500. The mean over all frequencies of the resulting variance error is calculated and compared to the theoretical variance (26). It is seen that for low n_1 and n_2 the theoretical variance is a good approximation. For example, up to about $n_1 = n_2 \approx 70$ the error from the theoretical value is less than 10%. However, for higher n_1, n_2 the approximation

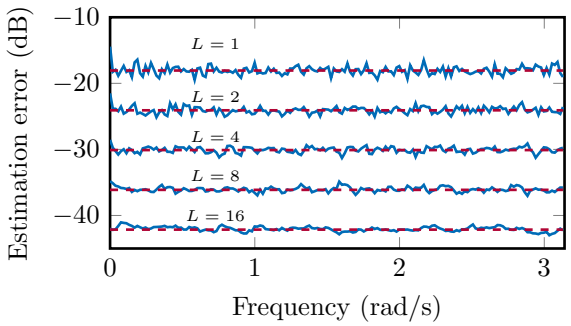

Fig. 5. Variance of FRF estimates for different local windows L. Simulated variance (——) and theoretical variance (- - -).

is insufficient and the variance is heavily influenced also by the choice of n_1 and n_2.

6.3 General System

In this section we study the estimation error for a more general system. The amplitude plot of the system is shown in Figure 7. The input signal is white Gaussian noise with unit variance, the disturbance noise is l also white noise with unit variance, and $N = 2000$ data samples are used. We use $n_1 = n_2 = 10$ and we vary L from 1 to 20 and check the bias and the mean square error. For

each value of L, 500 Monte-Carlo simulations are performed with a new input and noise realization in each simulation. Hence, we calculate the error over both noise and input realizations. In Figure 6 the bias at three specific frequencies are shown together with the theoretical values from Theorem 4. The first two frequencies are at the two resonance peaks ($\omega = 0.49$ and $\omega = 1.50$) and the third one is at frequency $\omega = 1.13$ in between the two resonance peaks. In this setup the local window width used in TRIMM is contained in the $3\,dB$ bandwidth of the first resonance peak for $L \lesssim 17$. Thus we expect from Theorem 4 that the bias error should grow as $O(L^2)$ for $L \lesssim 17$. The bias in the first resonance peak is closely matched for L up to about 15. For $L > 15$ the error is no longer expected to grow as $(2L)^2$. For the other two frequency points the $3\,dB$ bandwidth is much larger than 20 and hence $B_{\text{TRIMM}} < B_{3\text{dB}}$ for all values of L shown in Figure 6. The correspondence between simulated and theoretical values of the bias error is reasonably good, except for low values of L. One possible explanation is that in the proofs of the bias expressions we have used approximations like $L(L+1) \approx L^2$ that are not valid for small L.

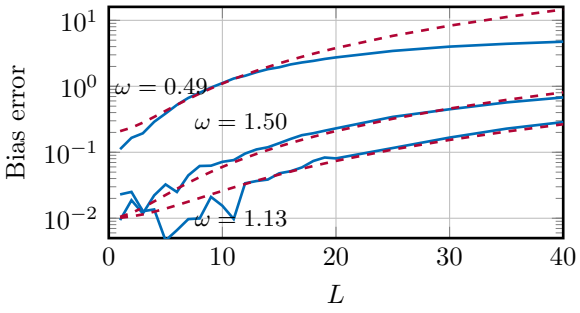

Fig. 6. The bias error in three different frequencies as a function of the local bandwidth of TRIMM. Simulated bias (——) and theoretical bias $O\left((2L)^2\right)$ (- - -)

In Figure 7 the mean over the Monte-Carlo simulations of the squared estimation error at each frequency is shown for five different values of L. It is seen that around the resonance peak the error increases as L is increased, indicating that around this frequency the bias error dominates. For other frequencies the error decreases as L increases. Here, the variance error dominates over the bias error since the $3\,dB$ bandwidth is high in these frequencies. Furthermore, the errors around the resonance peak increase proportionately to $(2L)^2$, where the bias error is dominating, while the errors in the other frequencies drop like $1/2L$, where the variance error dominates, agreeing with what is expected from Theorem 4 and the discussions on the variance in Section 4.2.

7 Experimental Illustration

In this section we will demonstrate the applicability of the TRIMM method to a real life problem. This small

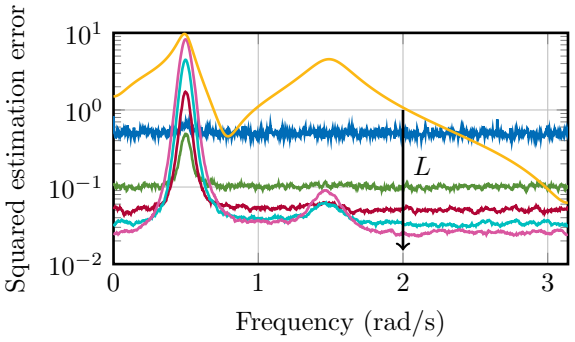

Fig. 7. The mean of the squared estimation error for $L = 1, 5, 10, 15, 20$. True system is shown as (——) and the arrow indicates increasing L.

example and the experimental data is taken from the vibrating steel beam example in [16]. The system has very low damping which generates long transient effects. The beam is excited by a mini-shaker and the excitation signal is generated by a waveform generator. The applied force to the beam and acceleration of the beam are measured. The objective of the experiment is to find a model from the force input to the acceleration of the steel beam. For a more detailed description of the experimental setup, see [16]. In the analysis of the TRIMM method in this paper we have assumed that the input is exactly known. However, in this example the force input is measured and it is therefore contaminated with noise. In [16] an instrumental variables approach was proposed as a remedy to this problem. Denoting the known reference signal from the waveform generator as $r(t)$, the input force $u(t)$ and the output $y(t)$, an estimate of the frequency response function from force to the acceleration is given by

$$\hat{G}_{yu}(\omega_k) = \frac{\hat{G}_{yr}(\omega_k)}{\hat{G}_{ur}(\omega_k)}, \tag{27}$$

where $\hat{G}_{yr}(\omega_k)$ and $\hat{G}_{ur}(\omega_k)$ are transfer function estimates from r to y and from r to u, respectively. Since the reference r is known exactly, it is possible to estimate the two transfer functions using TRIMM.

Two experiments are performed. In the first experiment the beam is excited with a periodic multisine excitation. The period of the multisine is $N = 1024$ points. A total of $M = 50$ periods of data are collected. These data will be used to find an estimate of the transfer function $\hat{G}_{yu}$ using (27). The two tranfer function estimates in (27) are calculated as

$$\hat{G}_{yr}^{(per)}(\omega_k) = \frac{\frac{1}{M}\sum_{i=1}^{M} Y^{[i]}(k)}{\frac{1}{M}\sum_{i=1}^{M} R^{[i]}(k)}$$

where the index $^{[i]}$ indicates the DFT spectrum from the i:th period of the data. The estimate $\hat{G}_{ur}(\omega_k)$ is calcu-

lated in the same way. In the estimation of the transfer functions only the last $M = 36$ periods are actually used. This is done to remove the effects of the initial transient. This gives a highly accurate estimate of the transfer function that will be used for comparison with TRIMM. For more details, see [16].

In the second experiment the system is excited with a random binary reference signal with the same length as the periodic signal. From this data we will estimate the transfer function using TRIMM. The parameters n_1 and n_2 are chosen as $n_1 = n_2 = 18$. Three different tunings of the TRIMM window width L will be used: $L = 2$, $L = 32$ and $L = 70$. The results are shown for these three different window widths in Figure 8: the top figures show the results over the whole frequency axis, while in the bottom figures we focus our attention to the second resonance peak (located approximately at 940 Hz). For $L = 2$ the frequency response estimate is noisy but as L is increased it becomes increasingly smooth. The amplitude of the second resonance peak has highest amplitude for $L = 32$. Looking in more detail at the two transfer functions G_{yr} and G_{ur} (not shown here) it is seen that G_{yr} is smooth around the resonance frequency while G_{ur} has a small amplitude and is noisy around the same frequency. This is due to the fact that at the resonance frequency the system is very flexible and it is hard to inject power at this frequency. Hence we get a small signal to noise ratio in the measurement of the force u. As shown in the analysis in the paper the variance decreases but the bias increases when L is increased. Since we have poor SNR at the resonance frequency a relativly large L is needed. However, when L is increased to 70, the estimate of the magnitude of the frequency response is lower. This indicates that the bias error dominates and the estimate will be biased. Hence, $L = 32$ seems to be a good compromise between bias and variance error. This tuning also gives results that are close to the high accuracy estimate from the periodic data.

One interesting observation from the estimate using the periodic data is that some of the resonance peaks are not visible. This is due to that the period length is 50 times shorter than the random input sequence and hence the resolution is 50 times smaller. This makes it hard to estimate the peak values using periodic data. This demonstrates the strength of the new non-parametric methods in that they are able to produce higher resolution estimates while maintaining similar accuracy.

As a final remark, in this example we have used the same tuning when estimating both G_{yr} and G_{ur}. By using different tunings, the estimate of G_{yu} could potentially be improved.

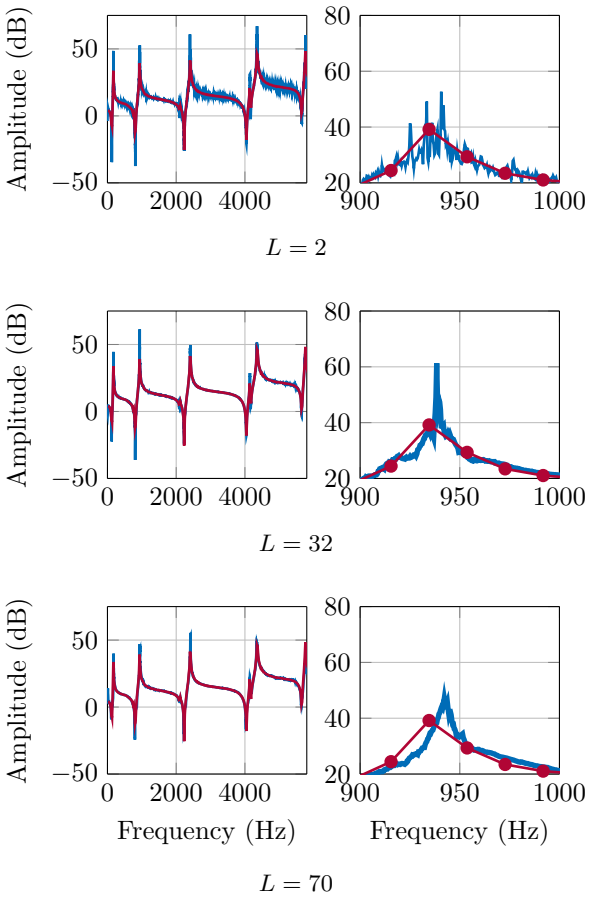

Fig. 8. The estimated frequency response function $\hat{G}_{yu}$ using TRIMM (——) and using the periodic data (—●—).

8 Conclusions

In this paper the bias and variance expressions for the estimation of the frequency response function using the TRIMM method was derived. The bias was studied first for a second order system with low damping since many systems can be written as sums of first and second order systems and the part with lowest damping dominates the error. The main observation is that the ratio between the local bandwidth used in TRIMM and the $3\,dB$ bandwidth of the system to a large extent decides the bias. The results are not only valid in the resonance peak of the system but can be used to understand the bias error for more general systems. That is, the bias error in each frequency is a function of the damping of the local dominating system in each particular frequency window. This analysis has allowed us to connect system properties and the choice of user parameters with the performance of the method.

The variance of the estimated FRF was also studied. The main result here is that if the user design parameters n_1 and n_2 are small compared to the number of samples, the variance will be proportional to the ratio between

the noise variance in the frequency and the input power over the local frequency window. The analysis in this paper is similar to the analysis of the Local Polynomial Method in [11,12,15]. This makes it easy to compare the performance of the different methods and give guidelines to the user when which method should be used and how. This is a topic for future research.

Another open question is how to estimate the noise spectrum with TRIMM. In some applications estimating the noise spectrum can be as important as estimating the FRF itself, see for example [14]. In [3] one way to estimating the noise spectrum with TRIMM was presented, however, it is not clear that this is the optimal way.

In Section 7 we applied TRIMM to real data. In the example we focused on the tuning when looking at the second resonance peak only. It is not necessarily so that the tuning of the parameters that are good around this resonance peak are good around other frequencies. This is a weakness of the TRIMM method compared to LPM, for example, that is completely local and where the estimates are independent in the different frequency windows. This being said, it should be possible to make TRIMM local by estimating new parameters in each frequency window; however this is a topic for future research.

Acknowledgements

This work was partially supported by the European Research Council under the European Community's Seventh Framework Programme (FP7/2007-2013) / ERC Grant Agreement No. 267381, the Swedish Research Council, the Linnaeus Center ACCESS at KTH, the Belgian Network DYSCO (Dynamical Systems, Control, and Optimization), funded by the Interuniversity Attraction Poles Programme initiated by the Belgian Science Policy Office, the Fund for Scientific Research (FWO-Vlaanderen), by the Flemish Government (Methusalem), and the Belgian Government through the Inter university Poles of Attraction (IAP VII) Program.

References

[1] D.R. Brillinger. *Time Series: Data Analysis, Forecasting and Control*. Holden-Day, San Francisco, California, 1981.

[2] M. Gevers, R. Pintelon, and Johan Schoukens. The local polynomial method for nonparametric system identification: Improvements and experimentation. In *Decision and Control and European Control Conference (CDC-ECC), 2011 50th IEEE Conference on*, pages 4302–4307, Dec 2011.

[3] Michel Gevers, Per Hägg, Håkan Hjalmarsson, Rik Pintelon, and Johan Schoukens. The transient impulse response modeling method and the local polynomial method for nonparametric system identification system identification. In *16th IFAC Symposium on System Identification*, volume 16, pages 55–60, 2012.

[4] P. Hägg, H. Hjalmarsson, and B. Wahlberg. A least squares approach to direct frequency response estimation. In *Decision and Control and European Control Conference (CDC-ECC), 2011 50th IEEE Conference on*, pages 2160–2165, Dec 2011.

[5] Per Hägg and Håkan Hjalmarsson. Non-parametric frequency function estimation using transient impulse response modelling. In *16th IFAC Symposium on System Identification*, pages 43–48, 2012.

[6] Per Hägg, Johan Schoukens, Michel Gevers, and Håkan Hjalmarsson. Addendum to "The transient impulse response modeling method for non-parametric system identification". *Availiable online at www.CHANGEME.com/TEST/TEST.pdf*, 2016.

[7] Lennart Ljung. *System identification : theory for the user*. Prentice Hall, Upper Saddle River, N.J., 2. ed. edition, 1999.

[8] Tomas McKelvey. Frequency domain identification. In *Preprints of the 12th IFAC Symposium on System Identification, Santa Barbara, USA.*, 2000.

[9] Tomas McKelvey and Guillaume Guérin. Non-parametric frequency response estimation using a local rational model. In *16th IFAC Symposium on System Identification*, volume 16, pages 49–54, 2012.

[10] R. Pintelon, J. Schoukens, and G. Vandersteen. Frequency domain system identification using arbitrary signals. *Automatic Control, IEEE Transactions on*, 42(12):1717 – 1720, December 1997.

[11] R. Pintelon, J. Schoukens, G. Vandersteen, and K. Barbé. Estimation of nonparametric noise and FRF models for multivariable systems–Part I: Theory. *Mechanical Systems and Signal Processing*, 24(3):573 – 595, 2010.

[12] R. Pintelon, J. Schoukens, G. Vandersteen, and K. Barbé. Estimation of nonparametric noise and FRF models for multivariable systems–Part II: Extensions, applications. *Mechanical Systems and Signal Processing*, 24(3):596 – 616, 2010.

[13] Rik Pintelon and Johan Schoukens. *System identification : a frequency domain approach*. IEEE Press, New York, 2001.

[14] J. Schoukens, Y. Rolain, G. Vandersteen, and R. Pintelon. User friendly box-jenkins identification using nonparametric noise models. In *Decision and Control and European Control Conference (CDC-ECC), 2011 50th IEEE Conference on*, pages 2148–2153, Dec 2011.

[15] J. Schoukens, G. Vandersteen, R. Pintelon, Z. Emedi, and Y. Rolain. Bounding the polynomial approximation errors of frequency response functions. *Instrumentation and Measurement, IEEE Transactions on*, 62(5):1346–1353, May 2013.

[16] Johan Schoukens, Gerd Vandersteen, Kurt Barbé, and Rik Pintelon. Nonparametric preprocessing in system identification: a powerful tool. *European Journal of Control*, 3-4:260–274, 2009.

[17] Petre Stoica and Randolph Moses. *Spectral analysis of signals*. Pearson Prentice Hall, Upper Saddle River, N.J., 2005.

A Regressor matrices for the least squares problem (13)

The regressor matrices for the extended input–output vector (11) used in the least squares problem (13), are

given by

$$\Phi_1 = \begin{bmatrix} \bar{U}_0 & & 0 \\ & \bar{U}_1 & \\ & \ddots & \\ 0 & & \bar{U}_{N-1} \end{bmatrix}, \quad \Phi_2 = \begin{bmatrix} \Phi_a & \Phi_b \end{bmatrix}, \quad \text{(A.1)}$$

where $\bar{U}_k = [U_{k-L}, \ldots, U_{k+L}]^T$ is a vector of the inputs in the frequency window around ω_k and

$$\Phi_a = \begin{bmatrix} \frac{1}{\sqrt{N}} & \frac{1}{\sqrt{N}} e^{-j\omega_{0-L}} & \cdots & \frac{1}{\sqrt{N}} e^{-j\omega_{0-L} n_1} \\ \vdots & \vdots & & \vdots \\ \frac{1}{\sqrt{N}} & \frac{1}{\sqrt{N}} e^{-j\omega_{N-1+L}} & \cdots & \frac{1}{\sqrt{N}} e^{-j\omega_{N-1+L} n_1} \end{bmatrix},$$

$$\Phi_b = \begin{bmatrix} \phi(0,-L,1) & \cdots & \phi(0,-L,n_2) \\ \vdots & & \vdots \\ \phi(N-1,L,1) & \cdots & \phi(N-1,L,n_2) \end{bmatrix}.$$

where $\phi(k,m,n) = \left(e^{-j\omega_{k+m} n} - e^{-j\omega_k n}\right) U_{k+m}$.

B Approximation error

The approximation error (12) for the system (17) can be written as

$$\begin{aligned} E_{n+r} &= \frac{1}{\sqrt{N}} \sum_{t=n_1}^{N-1} CA^t (I - A^N)^{-1} e^{-j\omega_{n+r} t} (x_0 - x_N) \\ &+ \sum_{t=n_2+1}^{N-1} \tilde{g}(t) \left(e^{-j\omega_{n+r} t} - e^{-j\omega_n t}\right) U_{n+r} \\ &= \frac{bp}{\sqrt{N}} \frac{1}{1-\lambda^N} \sum_{t=n_1}^{N-1} \lambda^t e^{j\omega_n t} e^{-j\omega_{n+r} t} (x_0 - x_N) \\ &+ b \sum_{p=0}^{\infty} \lambda^{pN} \sum_{t=n_2+1}^{N-1} \lambda^t \left(e^{-j\omega_r t} - 1\right) U_{n+r} \\ &= \frac{bp}{\sqrt{N}} \frac{1}{1-\lambda^N} \frac{\lambda^{n_1} e^{-j\omega_r n_1} - \lambda^N}{1 - \lambda e^{-j\omega_r}} (x_0 - x_N) \\ &+ \frac{bU_{n+r}}{1-\lambda^N} \left(\frac{\lambda^N - \lambda^{n_2+1}}{1-\lambda} - \frac{\lambda^N - \lambda^{n_2+1} e^{-j\omega_r (n_2+1)}}{1 - \lambda e^{-j\omega_r}} \right). \end{aligned}$$

C Technical Lemmas

Lemma 6 *Let $\frac{\sqrt{2}}{\sigma_u} U_k = X_k + jY_k$ for $k = 0, \ldots, N-1$ be zero mean, independent complex normally distributed, random variables with covariance*

$$E\left\{ \begin{bmatrix} X_k \\ Y_k \end{bmatrix} \begin{bmatrix} X_k & Y_k \end{bmatrix} \right\} = I$$

then

(1)

$$E\left\{ \frac{U_{k+q}^* U_k}{\sum_{r=-L}^{L} |U_{k+r}|^2} \right\} = \begin{cases} \frac{1}{2L+1} & \text{if } q = 0 \\ 0 & \text{otherwise} \end{cases}$$

(2)

$$E\left\{ \frac{U_{k+q}^*}{\sum_{r=-L}^{L} |U_{k+r}|^2} \right\} = 0$$

(3)

$$E\left\{ \frac{1}{\sum_{r=-L}^{L} |U_{k+r}|^2} \right\} = \frac{1}{\sigma_u^2} \frac{1}{2L}$$

PROOF. To save space, the proof is given in [6].

Lemma 7 *Let $\frac{\sqrt{2}}{\sigma_u} U_k$ be a sequence of independent complex random variables with distribution $\frac{\sqrt{2}}{\sigma_u} U_k \sim \mathcal{CN}\left(\begin{bmatrix} 0 \\ 0 \end{bmatrix}, \begin{bmatrix} 1 & 0 \\ 0 & 1 \end{bmatrix} \right)$ for $k = 0, \ldots, N-1$. Furthermore let x_0 be an given initial state of the system (2) and let x_N be the final state when the corresponding time realization $u(t) = \frac{1}{\sqrt{N}} \sum_{k=0}^{N-1} U_k e^{j\omega_k t}, t = 0, \ldots, N-1$ is applied to the system (2). It then holds that*

$$\begin{aligned} E\left\{ \frac{U_{k+q}^* (x_0 - x_N)}{\sum_{r=-L}^{L} |U_{k+r}|^2} \right\} = \\ - \frac{1}{(2L+1)\sqrt{N}} \sum_{\tau=0}^{N-1} A^{N-\tau-1} B e^{j\omega_{k+r}\tau}. \end{aligned}$$

PROOF. The proof is based on straighforward calculations using the relation between the final state of the system and the input sequnce and application of Lemma 6. The complete proof can be found in [6].

D Proof of Theorem 4

Using the structure of Φ_1, see (A.1), it can be shown that the bias at a frequency ω_k is given by

$$E\left\{ \hat{G}_k - G_k^{(0)} \right\} = E\left\{ \frac{\sum_{r=-L}^{L} U_{k+r}^* E_{k+r}}{\sum_{q=-L}^{L} |U_{k+q}|^2} \right\}. \quad \text{(D.1)}$$

We will now look at the specific frequency ω_n where the approximation error E_{n+r} is given by (18). Inserting the

approximation error (18) into (D.1) gives

$$
\begin{aligned}
&E\left\{\hat{G}_n - G_n^{(0)}\right\} = \\
&\sum_{r=-L}^{L} \frac{bp}{\sqrt{N}} \frac{1}{1-\lambda^N} \frac{\lambda^{n_1} e^{-j\omega_r n_1} - \lambda^N}{1-\lambda e^{-j\omega_r}} E\left\{\frac{U_{n+r}^*(x_0 - x_N)}{\sum_{r=-L}^{L} |U_{n+r}|^2}\right\} \\
&+ \sum_{r=-L}^{L} \frac{b}{1-\lambda^N} \left(\frac{\lambda^N - \lambda^{n_2+1}}{1-\lambda} - \frac{\lambda^N - \lambda^{n_2+1} e^{-j\omega_r(n_2+1)}}{1-\lambda e^{-j\omega_r}}\right) \\
&\times E\left\{\frac{|U_{n+r}|^2}{\sum_{r=-L}^{L} |U_{n+r}|^2}\right\}.
\end{aligned} \tag{D.2}
$$

Note that the first term in (D.2) stems from the undermodeling of the transient while the second term stems from the undemodeling of the impulse response.

The two expected values in (D.2) are given by Lemma 7 and Lemma 6, respectively. For the system with low damping (17), the bias (D.2) can be written as

$$
\begin{aligned}
&E\left\{\hat{G}_n - G_n^{(0)}\right\} \\
&= -\sum_{r=-L}^{L} \frac{bp}{\sqrt{N}} \frac{1}{1-\lambda^N} \frac{\lambda^{n_1} e^{-j\omega_r n_1} - \lambda^N}{1-\lambda e^{-j\omega_r}} \frac{1}{(2L+1)\sqrt{N}} \\
&\quad \times \sum_{\tau=0}^{N-1} \lambda^{N-\tau-1} e^{j\omega_n(N-\tau-1)} e^{j\omega_{n+r}\tau} \\
&\quad + \sum_{r=-L}^{L} \frac{b}{1-\lambda^N} \frac{1}{2L+1} \\
&\quad \times \left(\frac{\lambda^N - \lambda^{n_2+1}}{1-\lambda} - \frac{\lambda^N - \lambda^{n_2+1} e^{-j\omega_r(n_2+1)}}{1-\lambda e^{-j\omega_r}}\right) \\
&= -\frac{bpe^{-j\omega_n}}{(2L+1)N} \frac{1}{1-\lambda^N} \\
&\quad \times \sum_{r=-L}^{L} \frac{\lambda^{n_1} e^{-j\omega_r n_1} - \lambda^N}{1-\lambda e^{-j\omega_r}} \frac{1-\lambda^N}{1-\lambda e^{-j\omega_r}} e^{-j\omega_r} \\
&\quad + \frac{b}{1-\lambda^N} \frac{1}{2L+1} \\
&\quad \times \sum_{r=-L}^{L} \left(\frac{\lambda^N - \lambda^{n_2+1}}{1-\lambda} - \frac{\lambda^N - \lambda^{n_2+1} e^{-j\omega_r(n_2+1)}}{1-\lambda e^{-j\omega_r}}\right) \\
&= \frac{bpe^{-j\omega_n}}{(2L+1)N} \sum_{r=-L}^{L} \frac{\lambda^N - \lambda^{n_1} e^{-j\omega_r n_1}}{(1-\lambda e^{-j\omega_r})^2} e^{-j\omega_r} \\
&\quad + \frac{b}{1-\lambda^N} \frac{1}{2L+1} \\
&\quad \times \sum_{r=-L}^{L} \left(\frac{\lambda^N - \lambda^{n_2+1}}{1-\lambda} - \frac{\lambda^N - \lambda^{n_2+1} e^{-j\omega_r(n_2+1)}}{1-\lambda e^{-j\omega_r}}\right).
\end{aligned} \tag{D.3}
$$

By Assumption 2 gives $L \ll N$. Furthermore, we have assumed that the damping ϵ is small. This implies that

$$
\begin{aligned}
&1 - \lambda e^{-j\omega_r} \approx 1 - (1-\epsilon)(1-j\omega_r) = \\
&\epsilon + j\omega_r - j\omega_r\epsilon \approx \epsilon + j\omega_r, \quad \text{for } r = -L, \ldots, L.
\end{aligned} \tag{D.4}
$$

Hence the bias expression (D.3) can be written as

$$
\begin{aligned}
&\frac{bpe^{-j\omega_n}}{(2L+1)N} \sum_{r=-L}^{L} \frac{\lambda^N - \lambda^{n_1} e^{-j\omega_r n_1}}{(\epsilon + j\omega_r)^2} e^{-j\omega_r} \\
&+ \frac{b}{1-\lambda^N} \frac{1}{2L+1} \\
&\times \sum_{r=-L}^{L} \left(\frac{\lambda^N - \lambda^{n_2+1}}{\epsilon} - \frac{\lambda^N - \lambda^{n_2+1} e^{-j\omega_r(n_2+1)}}{\epsilon + j\omega_r}\right).
\end{aligned} \tag{D.5}
$$

We will now study the bias expression (D.5) for two different cases.

D.1 The case when $\epsilon < \frac{2\pi}{N}$

In this first case, we assume that $\epsilon < \frac{2\pi}{N}$ and it follows that $|\epsilon| < |\omega_r| = \frac{2\pi}{N}|r|$ for $r \neq 0$. Hence the dominating term in the first sum in (D.5) is obtained for $r = 0$ since

$$
\left|\frac{1}{\epsilon^2}\right| > \left|\frac{1}{(\epsilon + j\omega_r)^2}\right| \quad \text{for } r \neq 0.
$$

The terms of the second sum in (D.5) is zero for $r = 0$. Since $|\epsilon| < |\omega_r|$ for $r \neq 0$, these terms can be approximated as

$$
\left(\frac{\lambda^N - \lambda^{n_2+1}}{\epsilon} - \frac{\lambda^N - \lambda^{n_2+1} e^{-j\omega_r(n_2+1)}}{\epsilon + j\omega_r}\right) \approx \frac{\lambda^N - \lambda^{n_2+1}}{\epsilon}.
$$

Hence the bias (D.5) can be approximated as

$$
\begin{aligned}
E\left\{\hat{G}_n - G_n^{(0)}\right\} \approx &\frac{bpe^{-j\omega_n}}{(2L+1)N} \frac{\lambda^N - \lambda^{n_1}}{\epsilon^2} \\
&+ \frac{b}{1-\lambda^N} \frac{2L}{2L+1} \frac{\lambda^N - \lambda^{n_2+1}}{\epsilon}.
\end{aligned}
$$

Furthermore, since $\epsilon \ll 1$ we also have

$$
\lambda^n = (1-\epsilon)^n \approx 1 - n\epsilon,
$$

and

$$
\begin{aligned}
E\left\{\hat{G}_n - G_n^{(0)}\right\} \approx & \frac{bpe^{-j\omega_n}}{(2L+1)N}\frac{(1-N\epsilon)-(1-n_1\epsilon)}{\epsilon^2} \\
& + \frac{b}{1-(1-N\epsilon)}\frac{(1-N\epsilon)-(1-(n_2+1)\epsilon)}{\epsilon} \\
= & \frac{bpe^{-j\omega_n}}{2L+1}\frac{n_1-N}{N\epsilon} + b\frac{(n_2+1)-N}{N\epsilon} \\
= & \frac{1}{2L+1}O\left(\frac{n_1-N}{N\epsilon}\right) + O\left(\frac{(n_2+1)-N}{N\epsilon}\right). \qquad \square
\end{aligned}
$$

D.2 The case when $\epsilon > \frac{2\pi}{N}L$

The second case is when $\epsilon > \frac{2\pi}{N}L$, or equivalently, when $B_{3\text{dB}} > B_{\text{TRIMM}}$. Again we start from the expression of the bias (D.5).

First consider the bias contribution from the undermodeling of the transient:

$$
\frac{bpe^{-j\omega_n}}{(2L+1)N}\sum_{r=-L}^{L}\frac{\lambda^N - \lambda^{n_1}e^{-j\omega_r n_1}}{(\epsilon+j\omega_r)^2}e^{-j\omega_r}. \tag{D.6}
$$

In the considered case $\epsilon > \frac{2\pi}{N}L = \omega_L$ and we make the approximation $\epsilon + j\omega_r \approx \epsilon$ for $r = -L, \ldots, L$. The contribution to the bias (D.6) can thus be approximated as

$$
\begin{aligned}
& \frac{bpe^{-j\omega_n}}{(2L+1)N}\sum_{r=-L}^{L}\frac{\lambda^N - \lambda^{n_1}e^{-j\omega_r n_1}}{\epsilon^2}e^{-j\omega_r} \\
& = \frac{bpe^{-j\omega_n}}{(2L+1)N\epsilon^2}\left(\frac{\lambda^N(e^{-j\omega_L} - e^{j\omega_{L+1}})}{e^{j\omega_1}-1}\right. \\
& \quad \left. - \frac{\lambda^{n_1}(e^{-j\omega_L(n_1+1)} - e^{j\omega_{L+1}(n_1+1)})}{e^{j\omega_1(n_1+1)}-1}\right),
\end{aligned} \tag{D.7}
$$

where $\omega_1 = \frac{2\pi}{N}$. Since $L \ll N$, the first term of (D.7) can be approximated accurately by

$$
\begin{aligned}
& \frac{\lambda^N(e^{-j\omega_L} - e^{j\omega_{L+1}})}{e^{j\omega_1}-1} = \\
& \lambda^N\frac{1-j\omega_L-(1+j\omega_{L+1})+O(\omega_L^2)}{1+j\omega_1+O(\omega_1^2)-1} = \lambda^N O(2L+1).
\end{aligned} \tag{D.8}
$$

The second term of (D.7) can, after some calculations, be written as

$$
\lambda^{n_1}\frac{(e^{-j\omega_L(n_1+1)} - e^{j\omega_{L+1}(n_1+1)})}{e^{j\omega_1(n_1+1)}-1}, = -\lambda^{n_1}\frac{\sin\frac{\omega_{2L+1}(n_1+1)}{2}}{\sin\frac{\omega_1(n_1+1)}{2}}. \tag{D.9}
$$

Straightforward calculations gives that the maximum of the term

$$
\frac{\sin\frac{\omega_{2L+1}(n_1+1)}{2}}{\sin\frac{\omega_1(n_1+1)}{2}}, \tag{D.10}
$$

is obtained at $n_1 = -1$ with the maximum value being $2L+1$. Furthermore, the term (D.10) is oscillating and decaying as n_1 is increased. However, the decay is slower than for λ^{n_1} and hence the decay of the term (D.9) is dominated by λ^{n_1}. The second term in (D.7) can thus be approximated as

$$
\frac{\lambda^{n_1}(e^{-j\omega_L(n+1)} - e^{j\omega_{L+1}(n_1+1)})}{e^{j\omega_1(n_1+1)}} \approx \lambda^{n_1}O(2L+1). \tag{D.11}
$$

Using (D.7), (D.8) and (D.11), the complete contribution to the bias due to the undermodeling of the transient, (D.6), is given by

$$
\begin{aligned}
& \frac{bpe^{-j\omega_n}}{(2L+1)N}\sum_{r=-L}^{L}\frac{\lambda^N - \lambda^{n_1}e^{-j\omega_r n_1}}{(1-\lambda e^{-j\omega_r})^2}e^{-j\omega_r} \approx \\
& \frac{bpe^{-j\omega_n}}{(2L+1)N\epsilon^2}\left(\lambda^N O(2L+1) - \lambda^{n_1}O(2L+1)\right) \\
& \approx \lambda^{n_1}O\left(\frac{1}{N\epsilon^2}\right) = \lambda^{n_1}O\left(\frac{1}{NB_{3\text{dB}}^2}\right),
\end{aligned} \tag{D.12}
$$

where the last approximation is due to that $\lambda^{n_1} \leq \lambda^N$ and thus λ^{n_1} is the dominating term.

Next we consider the bias contribution from the undermodeling of the impulse response. In this case the approximation (D.4) is insufficient as higher order terms in the Taylor approximation will be needed. Let us take a step back and instead work with the contribution to the bias due to the undermodeling of the impulse response given in (D.3). Some straightforward calculations, uti-

lizing $\lambda = 1-\epsilon$, gives (with scaling $\frac{b}{1-\lambda^N}\frac{1}{2L+1}$ removed)

$$\begin{aligned}
&\sum_{r=-L}^{L}\left(\frac{\lambda^N-\lambda^{n_2+1}}{1-\lambda}-\frac{\lambda^N-\lambda^{n_2+1}e^{-j\omega_r(n_2+1)}}{1-\lambda e^{-j\omega_r}}\right)\\
&=\sum_{r=-L}^{L}\left(\frac{\lambda^N-\lambda^{n_2+1}}{\epsilon}-\frac{\lambda^N-\lambda^{n_2+1}e^{-j\omega_r(n_2+1)}}{1-(1-\epsilon)e^{-j\omega_r}}\right)\\
&=\sum_{r=-L}^{L}\left(\frac{(\lambda^N-\lambda^{n_2+1})(1-(1-\epsilon)e^{-j\omega_r})}{\epsilon(1-(1-\epsilon)e^{-j\omega_r})}-\right.\\
&\qquad\left.\frac{\epsilon(\lambda^N-\lambda^{n_2+1}e^{-j\omega_r(n_2+1)})}{\epsilon(1-(1-\epsilon)e^{-j\omega_r})}\right)\\
&=\sum_{r=-L}^{L}\left(\frac{(\lambda^N-\lambda^{n_2+1})(1-e^{-j\omega_r})-\epsilon(\lambda^N(1-e^{-j\omega_r})}{\epsilon(1-(1-\epsilon)e^{-j\omega_r})}\right.\\
&\qquad\left.-\frac{\lambda^{n_2+1}e^{-j\omega_r}(1-e^{-j\omega_r n_2}))}{\epsilon(1-(1-\epsilon)e^{-j\omega_r})}\right).
\end{aligned}\tag{D.13}$$

Since ϵ is small by assumption, we can approximate the contribution (D.13) as

$$\frac{b}{1-\lambda^N}\frac{1}{2L+1}\sum_{r=-L}^{L}\left(\frac{(\lambda^N-\lambda^{n_2+1})(1-e^{-j\omega_r})}{\epsilon(1-(1-\epsilon)e^{-j\omega_r})}\right),\tag{D.14}$$

By Assumption 2, $L \ll N$ and we approximate $e^{-j\omega_r}$ with the second order Taylor series around $r=0$:

$$e^{-j\omega_r}=e^{-j\frac{2\pi}{N}r}\approx 1-j\frac{2\pi}{N}r+\left(j\frac{2\pi}{N}r\right)^2.$$

Hence, (D.14) can be approximated as

$$\begin{aligned}
&\frac{b}{1-\lambda^N}\frac{\lambda^N-\lambda^{n_2+1}}{2L+1}\sum_{r=-L}^{L}\frac{1-\left(1-j\frac{2\pi}{N}r+\left(j\frac{2\pi}{N}r\right)^2\right)}{\epsilon^2}\\
&\qquad=\frac{b}{1-\lambda^N}\frac{\lambda^N-\lambda^{n_2+1}}{(2L+1)\epsilon^2}\sum_{r=-L}^{L}j\frac{2\pi}{N}r+\left(\frac{2\pi}{N}r\right)^2.
\end{aligned}\tag{D.15}$$

Since the sum in (D.15) is symmetric around $r=0$, the even terms sum to zero and (D.15) can be written as

$$\begin{aligned}
&\frac{b}{1-\lambda^N}\frac{\lambda^N-\lambda^{n_2+1}}{(2L+1)\epsilon^2}\left(\frac{2\pi}{N}\right)^2\frac{L(L+1)(2L+1)}{3}\\
&=\frac{b}{1-\lambda^N}\frac{\lambda^N-\lambda^{n_2+1}}{\epsilon^2}\left(\frac{2\pi}{N}\right)^2\frac{L(L+1)}{3}\\
&=\frac{\lambda^N-\lambda^{n_2+1}}{1-\lambda^N}O\left(\left(\frac{B_{\text{TRIMM}}}{B_{\text{3dB}}}\right)^2\right).
\end{aligned}\tag{D.16}$$

To summarize, the complete bias expression is approximated by

$$\begin{aligned}
E\left\{\hat{G}_n-G_n^{(0)}\right\}\approx{}&\lambda^{n_1}O\left(\frac{1}{NB_{\text{3dB}}^2}\right)\\
&+\frac{\lambda^N-\lambda^{n_2+1}}{1-\lambda^N}O\left(\left(\frac{B_{\text{TRIMM}}}{B_{\text{3dB}}}\right)^2\right),
\end{aligned}$$

where the two terms stems from the undermodeling of the transient (D.12) and the impulse response (D.16).

E Proof of Theorem 5

The impulse response of the system is given by $g(t)=\alpha\lambda^t$. Note that this is a special case of the impulse response considered in the low damping case in Section 4.1.1, $g(t)=b\lambda^t e^{j\omega_n t}$, when $b=\alpha$ and $\omega_n=0$. The bias expression (D.3) is thus valid.

By the assumption $0<\lambda\ll 1$ we have $\lambda^N \ll \lambda^{n_1}$ and $\lambda^N \ll \lambda^{n_2+1}$ and we can approximate (D.3) as

$$\begin{aligned}
&-\frac{\alpha}{(2L+1)N}\sum_{r=-L}^{L}\lambda^{n_1}e^{-j\omega_r(n_1+1)}\\
&+\alpha\frac{1}{2L+1}\sum_{r=-L}^{L}\lambda^{n_2+1}\left(e^{-j\omega_r(n_2+1)}-1\right).
\end{aligned}\tag{E.1}$$

The terms $e^{-j\omega_r(n_1+1)}$ and $e^{-j\omega_r(n_2+1)}$ are approximated by Taylor series expansions around $r=0$ and the bias (E.1) can be simplified to

$$\begin{aligned}
&-\frac{\alpha}{(2L+1)N}\sum_{r=-L}^{L}\lambda^{n_1}O(1)\\
&+\alpha\frac{1}{2L+1}\sum_{r=-L}^{L}\lambda^{n_2+1}\left(1-j\omega_r(n_2+1)\right.\\
&\qquad\left.+O\left(\omega_r^2(n_2+1)^2\right)-1\right)\\
&=-\frac{\alpha}{(2L+1)N}\lambda^{n_1}O(2L+1)\\
&+\alpha\frac{1}{2L+1}\sum_{r=-L}^{L}\lambda^{n_2+1}O(\omega_r^2(n_2+1)^2)\\
&=\lambda^{n_1}O\left(\frac{1}{N}\right)+\frac{\alpha\lambda^{n_2+1}}{2L+1}O\left(\left(\frac{2\pi}{N}\right)^2L^3(n_2+1)^2)\right)\\
&=\lambda^{n_1}O\left(\frac{1}{N}\right)+\alpha\lambda^{n_2+1}O\left(\left(\frac{2\pi}{N}\right)^2L^2\right)\\
&=\lambda^{n_1}O\left(\frac{1}{N}\right)+\lambda^{n_2+1}O\left(B_{\text{TRIMM}}^2\right),
\end{aligned}\tag{E.2}$$

where $B_{\text{TRIMM}} \triangleq 2\frac{2\pi}{N}L$.